CO_2 Capture Materials

DOI: 10.1002/anie.201105109

Competition and Cooperativity in Carbon Dioxide Sorption by Amine-Functionalized Metal–Organic Frameworks**

Ramanathan Vaidhyanathan, Simon S. Iremonger, George K. H. Shimizu, Peter G. Boyd, Saman Alavi, and Tom K. Woo**

Alkylamines, such as monoethanolamine, are used to scrub CO_2 molecules from flue gas streams, however, as they form strong chemical bonds (85–105 kJ mol^{-1}), the post-capture recovery of the amine is energy-intensive (130–150 °C including heating the entire aqueous solution).[1] Alternatively, the use of less-basic amines, such as aryl amines, could favor strong physisorption (30–50 kJ mol^{-1}) with CO_2, rather than chemisorption.[2] This would mean a porous compound with such amine groups could give easy-on/easy-off reversible CO_2 capture balanced with selectivity. To obtain high efficiency at lower partial pressures, the material, along with having strong CO_2 binding sites, needs to have reasonable surface area for capacity. Metal–organic frameworks (MOFs) are widely studied for gas sorption owing to the ability to modify pore sizes, shapes, and surfaces. Functionalizing with specific interaction sites is being actively studied as a route to selective gas capture.[3]

Computational modeling can give tremendous insight to the sorption properties of a MOF.[4] We recently reported a zinc aminotriazolato oxalate MOF, $\{Zn_2(Atz)_2(ox)\}$ (**2**), exhibiting amine-lined pores and a high heat of adsorption for CO_2 (ca. 40 kJ mol^{-1}).[5] Further studies showed that the CO_2 binding sites could be located crystallographically. These data offered an exceptional opportunity to validate a suite of computational methods[6] to model not only the CO_2 isotherm, but also the locations of binding sites and role of specific interactions to the overall CO_2 binding enthalpy. The present study applies these methods to understanding CO_2 uptake in another MOF, $\{Zn_3(Atz)_3(PO_4)\}$ (**1**), that intuitively should give better CO_2 capture properties. In comparison to $\{Zn_2(Atz)_2(ox)\}$, only two-thirds of the number of trianionic phosphate groups are required to charge compensate $[Zn(Atz)]^+$ layers, so larger, amine-lined pores were anticipated and observed. Despite this, the CO_2 uptake (at 273 K) and heat of adsorption do not exceed those of **2**. The computational methods provide crucial insight to understanding these phenomena and demonstrate the wide spread applicability of such techniques to ascertain binding details in MOFs not directly accessible by experiment. Although the role of the amine functionalities in **1** is surprisingly diminished, the cooperative interactions between CO_2 molecules are found to augment overall binding by over 7 kJ mol^{-1}, a significant result for CO_2 capture in any porous material.

Solvothermal reaction of basic $ZnCO_3$ with 3-amino-1,2,4-triazole, H_3PO_4, and NH_4OH gave $\{Zn_3Atz_3(PO_4)(H_2O)_{3.5}\}$, $\mathbf{1}\cdot(H_2O)_{3.5}$, in both single-crystal and bulk phases (Supporting Information, Figure S1). The aminotriazole ligand has been employed to construct other MOFs,[7,8] including with Zn ions, but has not been extensively studied for CO_2 capture excepting **2**. $\mathbf{1}\cdot(H_2O)_{3.5}$ is made up of cationic Zn–Atz layers pillared by PO_4 anions to form a 3D porous network (Figure 1). The Zn(Atz) layers lie in the *ac* plane and contain three independent Zn ions and Atz ligands. No amine groups coordinate to Zn ions; ligation is exclusively through triazole nitrogen atoms. Pillaring of these layers by the phosphate ions results in a 3D network of pores (accounting for van der

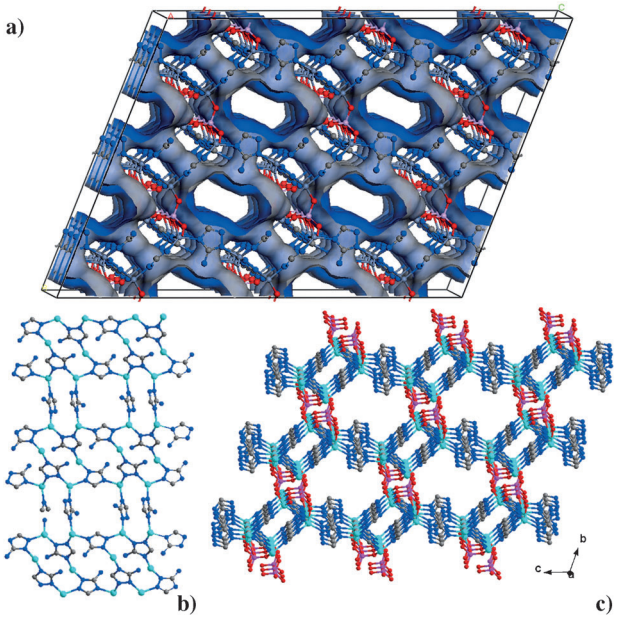

Figure 1. Structure of **1** (solvent molecules omitted for clarity). a) Connolly surface representation showing the three-dimensional structure of the Zn–Atz layers pillared by phosphate groups. b),c) Ball-and-stick representations showing the b) zinc–aminotriazolate layer and c) the structure showing the juxtapositioning of the Atz ligands. C gray, N dark blue, O red, P purple, Zn pale blue.

[*] Dr. R. Vaidhyanathan, Dr. S. S. Iremonger, Prof. G. K. H. Shimizu
Department of Chemistry, University of Calgary
Calgary T2N 1N4 (Canada)
E-mail: gshimizu@ucalgary.ca
P. G. Boyd, Dr. S. Alavi, Prof. T. K. Woo
Centre for Catalysis Research and Innovation
Department of Chemistry, University of Ottawa
Ottawa, K1N 6N5 (Canada)
E-mail: twoo@uottawa.ca

[**] The authors thank the Natural Sciences and Engineering Research Council of Canada, the Canada School for Energy and Environment, and the Canada Research Chairs Program for financial support.

Supporting information for this article is available on the WWW under http://dx.doi.org/10.1002/anie.201105109.

Waals radii: $a = 4.40 \times 6.55$, $b = 2.45 \times 2.78$ Å^2; [011] direction $= 2.66 \times 2.56$ Å^2). Thermogravimetric analysis of $\mathbf{1}\cdot(H_2O)_{3.5}$, showed a mass loss of 10.56% (calcd. 10.46% for 3.5 water molecules) from 25–150 °C, then a stable mass to 400 °C (Supporting Information, Figure S6), comparable to other reported Atz MOFs.[5,8]

PXRD of a sample subjected to 15 heating cycles to 60 °C under reduced pressure (ca. 10^{-6} mbar) showed that **1** retained crystallinity (Supporting Information, Figure S1). Adsorption studies on **1**, using CO_2, N_2, and H_2, showed uptakes of all gases studied (Figure 2; Supporting Information, Figure S7). A BET surface area of 470 $m^2 g^{-1}$ was calculated from 77 K N_2 isotherm. A surface area of 520 $m^2 g^{-1}$ and pore volume of 0.16 $cm^3 g^{-1}$ were calculated by DFT using the 273 K CO_2 isotherm (Supporting Information, Table S1). The heat of adsorption for CO_2, calculated using a Virial model using the 263 and 273 K adsorption isotherms (Supporting Information, Figures S8–S13),[8] was 32 kJ mol^{-1} at zero loading (Figure 2). This value is higher than most non-amine modified MOFs but significantly lower than the 40.8 kJ mol^{-1} observed in **2**.

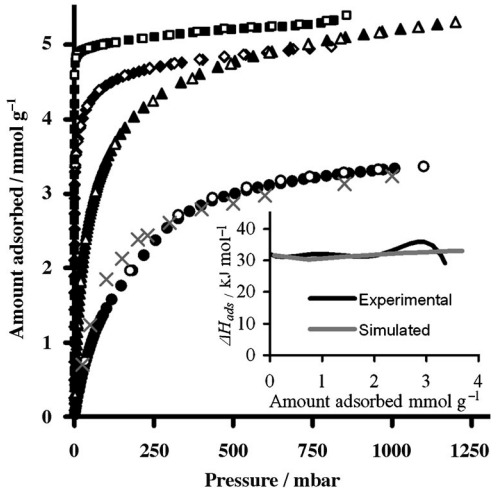

Figure 2. Sorption isotherms (adsorption: filled symbols, desorption: empty symbols) of **1** for CO_2 (273 K, ○; 195 K, ◇); N_2 (77 K, □); H_2 (77 K, △); simulated CO_2 adsorption isotherm at 273 K (×). Inset: Comparison of the simulated (determined from MD simulations at 273 K) and experimental (obtained from isotherms at 263 and 273 K) CO_2 enthalpy of adsorption of **1** as a function of guest loading.

The CO_2 uptake is considerably higher than observed in other reported Atz MOFs,[8c] but not as high as would have been expected in comparison to $\{Zn_2(Atz)_2(ox)\}$ (**2**). The pores in **1** are larger than those in **2** (3.5×4.0 Å^2; 3.9×2.1 Å^2; 3.0×1.6 Å^2),[5b] and given that **1** retains the available amine groups to enhance framework CO_2 interactions, higher CO_2 uptake was expected. Attempts to observe CO_2 crystallographically in **1** were not successful. A key structural feature extracted from the XRD data of the pure phase **1** was the buckling or staggered conformation of the ZnAtz layers (see Figure 1). The ZnAtz layer in **1** is corrugated, leading to juxtapositioning of adjacent Atz molecules in an antiparallel fashion. This results in the amines of **1** not protruding significantly into the pores. Quantitative analysis of the lower CO_2 uptake and ΔH_{ads} in **1** was provided computationally.

The CO_2 uptake of **1**, including isotherm, ΔH_{ads}, and location of CO_2 molecules, are modeled by a combination of classical grand canonical Monte Carlo (GCMC) simulations, molecular dynamics (MD) simulations, and periodic density functional theory (DFT) calculations.[6,10] This suite of techniques was validated on $\mathbf{2}\cdot(CO_2)_{0.8}$ and shown to accurately predict CO_2 binding sites.[5a] The inset in Figure 2 compares experimental and simulated CO_2 adsorption isotherms for **1** at 273 K. The simulated binding enthalpies shown in Figure 2 are calculated from the difference in the average potential energy resulting from 500 ps MD simulations. The overall agreement is excellent, but the simulated isotherm predicts slightly higher uptake than observed experimentally at low pressure. Figure 3 a,b show center-of-mass probability-density plots of CO_2 resulting from a GCMC simulation of **1** at 850 mbar and 273 K. The binding is dispersed in two regions, denoted α and β in Figure 3. The α regions are roughly parallel to the *ac* plane and located near the phosphate groups, while the β sites are roughly in the *bc* plane (the ZnAtz layer). The probability plots reveal that CO_2 molecules are not strongly localized, corroborating that CO_2 could not be located crystallographically in **1** as compared to **2**.

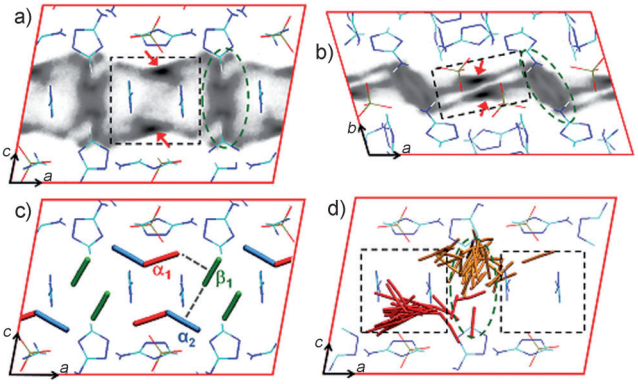

Figure 3. Centre-of-mass probability-density plots of CO_2 molecules in **1** at 273 K and 850 mbar pressure. Black dashed boxes: α region; green: β region. Shown are probability densities that are a) projected onto the *ac* plane, and b) projected onto the *ab* plane. c) Selected CO_2 binding-site geometries optimized at the DFT level. Symmetry-equivalent CO_2 molecules are represented in the same color. d) Trace of two CO_2 molecules (red and orange) during a 35 ps ab initio MD simulation of **1** at 273 K with a loading of four CO_2 molecules per unit cell (the other two CO_2 molecules are not shown). Thirty snapshots, separated by 1.2 ps, are depicted. For (a)–(d), a $2 \times 1 \times 1$ representation of the unit cell is shown that is shifted by 0.5 in the *a* direction in (d).

To locate the binding sites, CO_2 positions from the high probability regions were extracted from the GCMC simulations and optimized with dispersion corrected periodic DFT calculations. Three of these sites are given in Figure 3 c, where symmetry-equivalent sites are color-coded. The strongest binding site, α_1, matches the region of highest probability from the GCMC simulations (red arrows in Figure 3 a). Site α_1 was determined to have an empty framework binding enthalpy of 30.6 kJ mol^{-1} calculated with DFT, in good

agreement with the experimental zero loading ΔH_{ads} of 32 kJ mol^{-1}, but lower than the 39.6 kJ mol^{-1} calculated for the strongest binding site of **2**.

As the design premise of using the Atz ligands is that the amine groups enhance the CO_2 uptake, a widely accepted hypothesis, the amine–CO_2 binding was examined in more detail. Site α_1 has three amines in proximity with H_{amine}–O_{CO2} distances of 2.66, 2.83, and 3.26 Å. Using partial atomic charges derived from DFT calculations,[10,11] the electrostatic interactions between the amines with the CO_2 in a given binding site can be estimated. Interestingly, for α_1, this amine–CO_2 electrostatic interaction is found to be only −0.44 kJ mol^{-1}. For comparison, in **2**, the amine–CO_2 distances in the strongest binding site are longer (H_{amine}–O_{CO_2} = 2.72, 3.10, 3.68 Å), yet the amine-CO_2 electrostatic interaction is considerably more stabilizing at −5.4 kJ mol^{-1}. This is explained considering that, for α_1 in **1**, the CO_2–amine electrostatic interaction was attractive for two of the nearby amines (−0.02 and −2.39 kJ mol^{-1}) but repulsive for the other (+1.57 kJ mol^{-1}). For comparison, in **2**, all CO_2–amine interactions were attractive.

The analysis of the amine–CO_2 binding suggests that the densely grouped amines in **1** interfere with each other's ability to bind CO_2. It is important to note that this is only for a single binding site in **1**, and the binding sites are not as localized as in **2**. Nevertheless, the results suggest that the role of the amines in CO_2 binding in **1** is significantly diminished compared to **2**. To test this, we have simulated the isotherms of **1** and **2** replacing the amine groups with methyl groups in calculations. Methyl groups are isoelectronic with primary amine groups and so should have similar dispersion interactions, and are similar in size. However, as the two groups have different electron donating abilities, the resulting charge distributions should be quite distinct. Figure 4 shows the effect on CO_2 uptake of substituting the amines with methyl groups. In **1**, there is negligible difference in uptake upon substitution, consistent with the notion that the amines do not significantly contribute to the CO_2 binding. On the other hand, the same substitution gives a substantive decrease in **2** where CO_2 uptake decreases by about 20% over the pressure range examined.

Cooperative effects between CO_2 molecules have been recognized as contributing significantly to the overall heat of adsorption of CO_2,[12] particularly by Snurr et al.,[12a] and key to interpreting adsorption isotherm features. These effects were found to be significant in **2**[5a] and so were examined in **1** by studying the DFT-optimized binding sites. Cooperative binding is evinced in the strongest binding site in the β region of **1** (Figure 3c, labeled β_1). With an empty framework, the binding energy of β_1 is 29.0 kJ mol^{-1} at the DFT level. This energy increases to 32.0 kJ mol^{-1} when an adjacent α_1 site is occupied, implied by one of the dashed lines in Figure 3c. In examining the output configurations of the GCMC simulations, we found that an interesting triad of CO_2 molecules can form involving α_1, β_1, and α_2 (blue in Figure 3c). Within an empty framework, α_2 has a binding energy of 26.9 kJ mol^{-1}. However, as a $\alpha_1/\alpha_2/\beta_1$ triad, the average binding energy of the triad is 31.3 kJ mol^{-1} per CO_2 molecule. This is 7.4 kJ mol^{-1} more than the sum of the empty pore binding energies of α_1, α_2, and β_1. Adjacent α_1 and α_2 sites are mutually exclusive in that both cannot be occupied by CO_2 at the same time, shown as blue and red overlap in Figure 3c. Thus, it was thought that a CO_2 molecule in site α_1 (the most stable site) might occasionally slip into an adjacent α_2, to benefit from the favorable $\alpha_1/\alpha_2/\beta_1$ triad interactions. The stabilization imparted by an appropriately oriented T-shaped dimer of CO_2 molecules was estimated to be 3.9–4.6 kJ mol^{-1}.[5a] The value of 7.4 kJ mol^{-1} for a triad can lead one to postulate that appropriately oriented higher aggregates (T-shapes can further assemble into pinwheel tetrads or even infinite herring-bone arrays) will demonstrate pronounced cooperativity and enhanced heats of adsorption for CO_2. To examine the general mobility of CO_2 molecules in the pores, MD simulations of **1** at 273 K were performed.

As the unit cell of **1** is small, ab initio MD simulations were performed on a single unit cell with four CO_2 molecules at the same DFT-D level of theory used to evaluate the binding energies. Figure 3d shows two of four positions of CO_2 molecules resulting from a 35 ps MD simulation. The red CO_2 was initially in the α_1 site, whereas orange CO_2 was initially in the β region. Thirty successive snapshots, separated by 1.2 ps, are depicted. Figure 3d shows that the red CO_2 is generally localized to the α_1 site and the snapshots map a region similar to that in the GCMC probability distributions in Figure 3a. The trajectory shows that the CO_2 does slip into the α_2 site and even into the β region during the short simulation. When CO_2 slips into the α_2 site, snapshots of the MD simulation (not shown) indeed show the $\alpha_1/\alpha_2/\beta_1$ triad forming.

The ability to design better sorbent materials for CO_2 is a global issue. Three regimes for gas adsorption have been identified to operate under different conditions in MOFs. These are low pressure adsorption based on heat of adsorption (which is guided by functional groups in the material), medium pressure adsorption based on available surface area in the MOF, and high pressure adsorption based on available pore volume.[13] In the search for better low pressure CO_2 sorbent materials, amine functionalization of porous solids has been a common strategy. However, to obtain efficient CO_2 capture both the adsorption sites and the pore structure must be optimal. The present study expands the use of combined experiment and simulation methods to under-

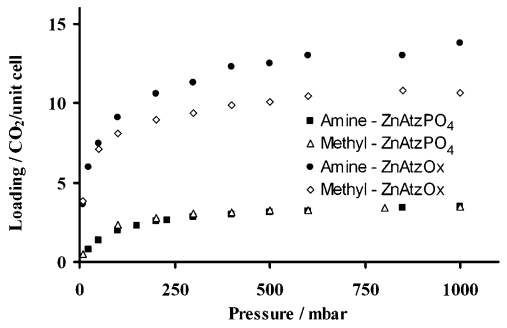

Figure 4. Simulated CO_2 adsorption isotherms for the phosphate **1**, the oxalate **2**, and their respective calculated methyl-for-amine substituted derivatives at 273 K.

standing subtleties in CO_2 binding in aminated solids. It emphasizes that higher degrees of amination are not necessarily favorable as excessive clustering of amine groups can, in fact, interfere with CO_2 binding. It also further affirms that cooperative interactions between CO_2 molecules contribute significantly to binding energies and it is postulated that sorbents with pores that bind higher aggregates of CO_2 will significantly enhance heats of adsorption.

Experimental Section

Synthesis of single crystals of $\{Zn_3(Atz)_3(PO_4)\}\cdot(H_2O)_{3.5}$ ($\mathbf{1}\cdot(H_2O)_{3.5}$): Colorless crystals of $\mathbf{1}\cdot(H_2O)_{3.5}$ in the shape of thick square plates were obtained from the reaction of a mixture containing $ZnCO_3\cdot 2\,Zn(OH)_2$ (0.1 g), H_3PO_4 (0.03 g), 3-amino-1,2,4-triazole (0.4 g), NH_4OH (30%, 0.08 mL), methanol (2 mL), and water (2 mL) at 180°C for 2 days (yield: ca. 70% based on zinc). Initial pH 8.0–8.5; final pH 6.5–7.0. Elemental analysis (%) calcd for $C_6H_{16}N_{12}O_{7.5}PZn_3$: C 11.94, H 2.67, N 27.86; found: C 11.97, H 2.70, N 27.83. The pH was crucial; anything below this pH resulted in the formation of a mixture of unidentified phases along with **1**. The crystals of $\mathbf{1}\cdot(H2O)_{3.5}$ grew as a crop of colorless crystals, which were mostly twinned and heavily intergrown, but a good single crystal was chosen. Our attempts to locate the CO_2 within the pores of **1** using single crystal X-ray diffraction experiments have so far been unsuccessful.

Additional powder X-ray diffraction details, additional gas sorption data including N_2 and H_2 isotherms for **1**, computational details of construction of the potential energy surface, and MD and GCMC simulations of **1**, including heat of adsorption calculations and comparison to **2**, are given in the Supporting Information.

CDC 782799 contains the supplementary crystallographic data for this paper. These data can be obtained free of charge from The Cambridge Crystallographic Data Centre via www.ccdc.cam.ac.uk/data_request/cif.

Received: July 21, 2011
Published online: December 23, 2011

Keywords: adsorption simulation · amines · carbon dioxide · metal–organic frameworks

[1] G. T. Rochelle, *Science* **2009**, *325*, 1652, and references therein.
[2] a) S. Couck, J. F. M. Denayer, G. V. Baron, T. Remy, J. Gascon, F. Kapteijn, *J. Am. Chem. Soc.* **2009**, *131*, 6326; b) B. Arstad, H. Fjellvåg, K. O. Kongshaug, O. Swang, R. Blom, *Adsorption* **2008**, *14*, 755; c) A. R. Millward, O. M. Yaghi, *J. Am. Chem. Soc.* **2005**, *127*, 17998.
[3] a) S. Keskin, T. M. van Heest, D. S. Sholl, *ChemSusChem* **2010**, *3*, 879; b) Y. Chen, J. Jiang, *ChemSusChem* **2010**, *3*, 982; c) J. An, S. J. Geib, N. L. Rosi, *J. Am. Chem. Soc.* **2010**, *132*, 38; d) K. Sumida, S. Horike, S. S. Kaye, Z. R. Herm, W. L. Queen, C. M. Brown, F. Grandjean, G. J. Long, A. Dailly, J. R. Long, *Chem. Sci.* **2010**, *1*, 184; e) B.-J. Lin, W. Xue, P.-J. Zhang, X.-M. Chen, *Chem. Commun.* **2011**, *47*, 926; f) D. M. D'Alessandro, B. Smit, J. R. Long, *Angew. Chem.* **2010**, *122*, 6194; *Angew. Chem. Int. Ed.* **2010**, *49*, 6058; g) R. Banerjee, H. Furukawa, D. Britt, C. Knobler, M. O'Keeffe, O. M. Yaghi, *J. Am. Chem. Soc.* **2009**, *131*, 3875; h) P. K. Thallapally, J. Tian, M. Radha Kishan, C. A. Fernandez, S. J. Dalgarno, P. B. McGrail, J. E. Warren, J. L. Atwood, *J. Am. Chem. Soc.* **2008**, *130*, 16842; i) D. Britt, H. Furukawa, B. Wang, T. G. Glover, O. M. Yaghi, *Proc. Natl. Acad. Sci. USA* **2009**, *106*, 20637; j) K. C. Stylianou, J. E. Warren, S. Y. Chong, J. Rabone, J. Bacsa, D. Bradshaw, M. J. Rosseinsky, *Chem. Commun.* **2011**, *47*, 3389; k) S. R. Caskey, A. G. Wong-Foy, A. J. Matzger, *J. Am. Chem. Soc.* **2008**, *130*, 10870; l) T. Panda, P. Pachfule, Y. F. Chen, J. W. Jiang, R. Banerjee, *Chem. Commun.* **2011**, *47*, 2011; m) Z. X. Chen, S. C. Xiang, H. D. Arman, P. Li, D. Y. Zhao, B. L. Chen, *Eur. J. Inorg. Chem.* **2011**, 2227; n) B.-J. Lin, W. Xue, P.-J. Zhang, X.-M. Chen, *J. Am. Chem. Soc.* **2010**, *132*, 6654.
[4] a) O. K. Farha, A. O. Yazaydin, I. Eryazici, C. D. Malliakas, B. G. Hauser, M. G. Kanatzidis, S. T. Nguyen, R. Q. Snurr, J. T. Hupp, *Nat. Chem.* **2010**, *2*, 944; b) Z. Xiang, D. Cao, J. Lan, W. Wang, D. P. Broom, *Energy Environ. Sci.* **2010**, *3*, 1469; c) A. O. Yazaydın, R. Q. Snurr, H.-T. Park, K. Koh, J. Liu, M. D. LeVan, A. I. Benin, P. Jakubczak, M. Lanuza, D. B. Galloway, J. J. Low, R. R. Willis, *J. Am. Chem. Soc.* **2009**, *131*, 18198; d) D. Farrusseng, C. Daniel, C. Gaudillere, U. Ravon, Y. Schuurman, C. Mirodatos, D. Dubbeldam, H. Frost, R. Q. Snurr, *Langmuir* **2009**, *25*, 7383; e) E. Stavitski, E. A. Pidko, S. Couck, T. Remy, E. J. M. Hensen, B. M. Weckhuysen, J. Denayer, J. Gascon, F. Kapteijn, *Langmuir* **2011**, *27*, 3970.
[5] a) R. Vaidhyanathan, S. S. Iremonger, G. K. H. Shimizu, P. G. Boyd, S. Alavi, T. K. Woo, *Science* **2010**, *330*, 650; b) R. Vaidhyanathan, S. S. Iremonger, K. W. Dawson, G. K. H. Shimizu, *Chem. Commun.* **2009**, 5230.
[6] a) T. Düren, Y. S. Bae, R. Q. Snurr, *Chem. Soc. Rev.* **2009**, *38*, 1237; b) B. Smit, T. L. M. Maesen, *Chem. Rev.* **2008**, *108*, 4125; c) M. Tafipolsky, S. Amirjalayer, R. Schmid, *Microporous Mesoporous Mater.* **2010**, *129*, 304.
[7] Y. Y. Lin, Y. B. Zhang, J. P. Zhang, X. M. Chen, *Cryst. Growth Des.* **2008**, *8*, 3673.
[8] a) C. Y. Su, A. M. Goforth, M. D. Smith, P. J. Pellechia, H. C. zur Loye, *J. Am. Chem. Soc.* **2008**, *130*, 3576; b) W. Li, H. P. Jia, Z. F. Ju, J. Zhang, *Cryst. Growth Des.* **2006**, *6*, 2136; c) H. Park, G. Krigsfeld, S. J. Teat, J. B. Parise, *Cryst. Growth Des.* **2007**, *7*, 1343; d) G.-Q. Zhai, C. Z. Lu, Y.-X. Wu, S. R. Batten, *Cryst. Growth Des.* **2007**, *7*, 2332.
[9] a) X. Zhao, S. Villar-Rodil, A. J. Fletcher, K. M. Thomas, *J. Phys. Chem. B* **2006**, *110*, 9947; b) X. B. Zhao, B. Xiao, A. J. Fletcher, K. M. Thomas, *J. Phys. Chem. B* **2005**, *109*, 8880; J. H. Cole, D. H. Everett, C. T. Marshall, A. R. Paniego, J. C. Powl, F. Rodriguez-Reinoso, *J. Chem. Soc. Faraday Trans.* **1974**, *70*, 2154; c) I. P. O'koye, M. Benham, K. M. Thomas, *Langmuir* **1997**, *13*, 4054; C. R. Reid, I. P. O'koye, K. M. Thomas, *Langmuir* **1998**, *14*, 2415; d) C. R. Reid, K. M. Thomas, *Langmuir* **1999**, *15*, 3206; e) C. R. Reid, K. M. Thomas, *J. Phys. Chem. B* **2001**, *105*, 10619.
[10] C. Campañá, B. Mussard, T. K. Woo, *J. Chem. Theory Comput.* **2009**, *5*, 2866.
[11] These are the same charges used for the GCMC simulations.
[12] a) K. S. Walton, A. R. Millward, D. Dubbeldam, H. Frost, J. J. Low, O. M. Yaghi, R. Q. Snurr, *J. Am. Chem. Soc.* **2008**, *130*, 406; b) K. L. Kauffman, J. T. Culp, A. Goodman, C. Matranga, *J. Phys. Chem. C* **2011**, *115*, 1857.
[13] H. Frost, T. Düren, R. Q. Snurr, *J. Phys. Chem. B* **2006**, *110*, 9565.

